Vortex-Trap-Induced Fusion of Femtoliter-Volume Aqueous Droplets

Robert M. Lorenz,[†] J. Scott Edgar,[†] Gavin D. M. Jeffries,[†] Yiqiong Zhao,[†] David McGloin,[‡] and Daniel T. Chiu*,[†]

Department of Chemistry, University of Washington, Seattle, Washington 98195-1700, and School of Physics and Astronomy, University of St. Andrews, North Haugh, St. Andrews, Fife KY16 9SS, UK

This paper describes the use of an optical vortex trap for the transport and fusion of single femtoliter-volume aqueous droplets. Individual droplets were generated by emulsifying water in acetophenone with SPAN 80 surfactant. We demonstrate the ability of optical vortex traps to position trapped droplets precisely while excluding surrounding aqueous droplets from entering the trap, thereby preventing unwanted cross contamination by other nearby droplets. Additionally, the limitation of optical vortex traps for inducing droplet fusion is illustrated, and a remedy is provided through modulation of the spatial intensity profile of the optical vortex beam. Spatial modulation was achieved by translating the computer-generated hologram (CGH) with respect to the input Gaussian beam, thereby shifting the location of the embedded phase singularity (dark core) within the optical vortex beam. We present both simulated and experimentally measured intensity profiles of the vortex beam caused by translation of the CGH. We further describe the use of this technique to achieve controlled and facile fusion of two aqueous droplets.

The appealing attributes of integrated functionality and precise control of small volumes have been realized recently with droplet-based microfluidics,[1–27] as evidenced by the number of techniques that have been demonstrated in the diverse areas of biological assays,[6,11–13] protein crystallization,[14,15] and chemical reactions.[1–4,8,16–19] Accompanying these systems is the need to sort and manipulate the generated droplets for collection or detection and in the case of synthesis or labeling reactions, droplet fusion will be necessary. This need has been addressed through channel design,[10,22] electrowetting,[4,9,13,23–25] and optical techniques.[7,11,26,27] Among optical techniques, optical trapping is a desirable choice for droplet control because it offers the benefits of easy implementation and use with microscopy setups and compatibility with any transparent chip design, while having an extensive history of use in the manipulation of single molecules, cells, and other particles coupled with high-sensitivity detection.[28,29]

Despite advantages conferred by optical trapping, there are some disadvantages when attempting to trap and fuse aqueous droplets. (1) Optical tweezers, the most common optical trapping technique, cannot be applied to the manipulation of aqueous droplets dispersed in an immiscible medium (with the exception of perfluoro solvents). Normally, high-refractive-index (RI) par-

* Author to whom correspondence should be addressed: E-mail: chiu@chem.washington.edu.

† University of Washington.

‡ University of St. Andrews.

(1) Lorenz, R. M.; Edgar, J. S.; Jeffries, G. D. M.; Chiu, D. T. *Anal. Chem.* **2006**, *78*, 6948–6954.

(2) Steinbacher, J. L.; Moy, R. W. Y.; Price, K. E.; Cummings, M. A.; Roychowdhury, C.; Buffy, J. J.; Olbricht, W. L.; Haaf, M.; McQuade, D. T. *J. Am. Chem. Soc.* **2006**, *128*, 9442–9447.

(3) Nie, Z.; Li, W.; Seo, M.; Xu, S.; Kumacheva, E. *J. Am. Chem. Soc.* **2006**, *128*, 9408–9412.

(4) Dubois, P.; Marchand, G.; Fouillet, Y.; Berthier, J.; Douki, T.; Hassine, F.; Gmouh, S.; Vaultier, M. *Anal. Chem.* **2006**, *78*, 4909–4917.

(5) Edgar, J. S.; Pabbati, C. P.; Lorenz, R. M.; He, M.; Fiorini, G. S.; Chiu, D. T. *Anal. Chem.* **2006**, *78*, 6433–6439.

(6) Song, H.; Li, H.-W.; Munson, M. S.; Ha, T. G. V.; Ismagilov, R. F. *Anal. Chem.* **2006**, *78*, 4839–4849.

(7) Reiner, J. E.; Crawford, A. M.; Kishore, R. B.; Goldner, L. S.; Helmerson, K.; Gilson, M. K. *Appl. Phys. Lett.* **2006**, *89*, 013904.

(8) Hung, L.-H.; Choi, K. M.; Tseng, W.-Y.; Tan, Y.-C.; Shea, K. J.; Lee, A. P. *Lab Chip* **2006**, *6*, 174–178.

(9) Wheeler, A. R.; Moon, H.; Bird, C. A.; Ogorzalek Loo, R. R.; Kim, C.-J.; Loo, J. A.; Garrell, R. L. *Anal. Chem.* **2005**, *77*, 534–540.

(10) Tan, Y.-C.; Lee, A. P. *Lab Chip* **2005**, *5*, 1178–1183.

(11) Kotz, K. T.; Gu, Y.; Faris, G. W. *J. Am. Chem. Soc.* **2005**, *127*, 5736–5737.

(12) He, M.; Edgar, J. S.; Jeffries, G. D. M.; Lorenz, R. M.; Shelby, J. P.; Chiu, D. T. *Anal. Chem.* **2005**, *77*, 1539–1544.

(13) Srinivasan, V.; Pamula, V. K.; Fair, R. B. *Lab Chip* **2004**, *4*, 310–315.

(14) Zheng, B.; Tice, J. D.; Ismagilov, R. F. *Adv. Mater.* (Weinheim, Ger.) **2004**, *16*, 1365–1368.

(15) Zheng, B.; Tice, J. D.; Roach, L. S.; Ismagilov, R. F. *Angew. Chem. Int. Ed.* **2004**, *43*, 2508–2511.

(16) Dendukuri, D.; Tsoi, K.; Hatton, T. A.; Doyle, P. S. *Langmuir* **2005**, *21*, 2113–2116.

(17) Chan, E. M.; Alivisatos, A. P.; Mathies, R. A. *J. Am. Chem. Soc.* **2005**, *127*, 13854–13861.

(18) Xu, S.; Nie, Z.; Seo, M.; Lewis, P.; Kumacheva, E.; Stone, H. A.; Garstecki, P.; Weibel, D. B.; Gitlin, I; Whitesides, G. M. *Angew. Chem. Int. Ed.* **2005**, *44*, 724–728.

(19) He, M.; Sun, C.; Chiu, D. T. *Anal. Chem.* **2004**, *76*, 1222–1227.

(20) He, M.; Kuo, J. S.; Chiu, D. T. *Langmuir* **2006**, *22*, 6408–6413.

(21) He, M.; Kuo, J. S.; Chiu, D. T. *Appl. Phys. Lett.* **2005**, *87*, 031916.

(22) Tan, Y.-C.; Fisher, J. S.; Lee, A. I.; Cristini, V.; Lee, A. P. *Lab Chip* **2004**, *4*, 292–298.

(23) Wheeler, A. R.; Moon, H.; Kim, C.-J.; Loo, J. A.; Garrell, R. L. *Anal. Chem.* **2004**, *76*, 4833–4838.

(24) Kuo, J. S.; Spicar-Mihalic, P.; Rodriguez, I.; Chiu, D. T. *Langmuir* **2003**, *19*, 250–255.

(25) Pollack, M. G.; Fair, R. B.; Shenderov, A. D. *Appl. Phys. Lett.* **2000**, *77*, 1725–1726.

(26) Kotz, K. T.; Noble, K. A.; Faris, G. W. *Appl. Phys. Lett.* **2004**, *85*, 2658–2660.

(27) Chiou, P. Y.; Moon, H.; Toshiyoshi, H.; Kim, C.-J.; Wu, M. C. *Sens. Actuators, A* **2003**, *A104*, 222–228.

(28) Grier, D. G. *Nature (London)* **2003**, *424*, 810–816.

(29) Kuyper, C. L.; Chiu, D. T. *Appl. Spectrosc.* **2002**, *56*, 300A.

PAGE EST: 4.6

ticles in a low-refractive-index medium are trapped, such as beads or cells dispersed in an aqueous buffer. Unfortunately, the RI for aqueous droplets (1.33) is invariably lower than the refractive index of the surrounding immiscible medium, and in this situation the aqueous droplets will be repelled by the optical tweezer. This limitation can be overcome by using vortex traps, which have a dark core.[30−32] (2) Perfluoro-type solvents (RI of ~1.29) are the only immiscible medium with an RI lower than that of water to our knowledge, which allows trapping with either optical tweezers or optical vortex traps. There are, however, two issues with the use of perfluoro solvents. First, we have been unable to form and maintain small femtoliter-volume aqueous droplets in perfluoro solvents using a microfluidic platform,[1] owing to the highly hydrophobic character of the perfluorinated oils. Second, it is difficult to trap selectively one aqueous droplet in the presence of other close-by droplets, because the optical tweezer tends to draw in any nearby droplets and thus leads to unwanted cross contamination by other droplets or unwanted fusion with other droplets.

Previously, we demonstrated the ability to increase the RI of aqueous droplets by concentrating the dissolved solutes within the droplets such that an optical tweezer could be employed to position and fuse the droplets; we also demonstrated the use of optical vortex traps to overcome the problems of trapping and manipulating aqueous droplets in nonfluorinated oil.[1] Although useful, changing the RI of the aqueous droplets may not always be compatible with the desired experiment, and the use of optical vortex traps, while enabling trapping of aqueous droplets in the immiscible medium, does not allow droplet fusion.

To address the obstacles inherent with the use of optical trapping and to achieve facile manipulation and fusion of aqueous droplets in immiscible media, this paper describes a technique based on the spatial modulation of optical vortex traps for the controlled fusion of single femtoliter-volume aqueous droplets. In contrast to other optical manipulation techniques, aqueous droplets can be trapped in any immiscible medium, transported, and controllably fused together. When used in nonfluorinated oils, enhanced stability and control are conferred by vortex trapping, because it repels all other aqueous droplets from the trapped droplet, thereby preventing unwanted droplet fusion and sample contamination. Our optical technique can be implemented into any transparent microfluidic chip, such as glass or polymer, and is especially well-suited for use with poly(dimethylsiloxane) (PDMS), which allows users to take advantage of the low cost and high yield bestowed by the established method of rapid prototyping.

EXPERIMENTAL SECTION

Generation and Spatial Modulation of Dual Optical Vortex Traps. Figure 1A depicts our experimental setup. The optical vortex trap was formed by passing the beam from the Nd:YAG laser through a computer-generated hologram (CGH), after which the Laguerre-Gaussian ($LG_p^{\pm L}$) mode was isolated and then
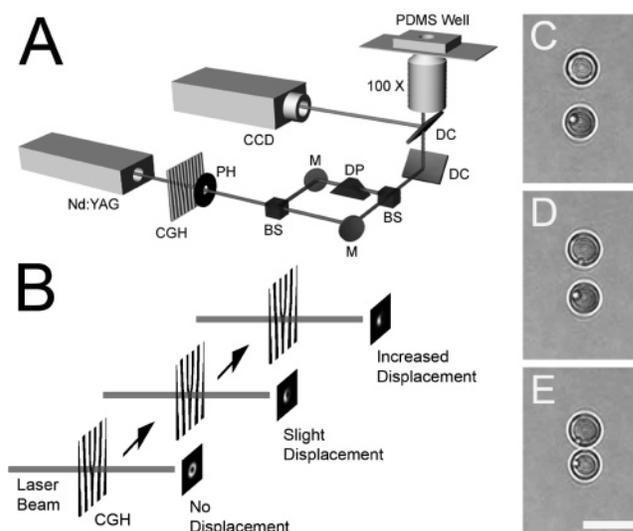
(30) Gahagan, K. T.; Swartzlander, G. A. *Opt. Lett.* **1996**, *21*, 827−829.
(31) Gahagan, K. T.; Swartzlander, G. A. *J. Opt. Soc. Am. B*−Opt. Phys. **1999**, *16*, 533−537.
(32) Prentice, P. A.; MacDonald, M. P.; Frank, T. G.; Cuschieri, A.; Spalding, G. C.; Sibbett, W.; Campbell, P. A.; Dholakia, K. *Opt. Exp.* **2004**, *12*, 593−600.

Figure 1. (A) Schematic outlining the experimental setup used to generate dual optical vortex traps for the manipulation and fusion of aqueous droplets. The TEM$_{00}$ output of the CW Nd:YAG laser was sent through a computer-generated hologram (CGH) to create a Laguerre-Gaussian (LG) beam, then spatially filtered through a pinhole (PH) before being split by a polarization beam splitter (BS) into two separate trapping beams. A dove prism (DP) was placed in the path of one of the beams to change the handedness of the beam for subsequent trapping. Both beams were then combined by a second polarization beam-splitting cube, prior to being sent into the back aperture of a high-numerical-aperture (NA = 1.3) objective. Abbreviations: CGH, computer-generated hologram; BS, beam-splitter; M, mirror; DP, dove prism; PH, pinhole; DC, dichroic mirror. (B) Schematic demonstrating the displacement of the CGH with respect to the laser beam, which caused a change in the spatial intensity profile of the optical vortex beam. Panels C−E demonstrate the optical trapping and placement of two aqueous droplets in acetophenone/SPAN 80 0.0025% w/w. The scale bar in (E) represents 10 μm.

spatially filtered. The beam generated was an LG_0^1, where L (the azimuthal mode index, which denotes the number of 2π phase cycles in a closed path about the beam axis and in turn the beam handedness) was 1 and index p (the index number of nonaxial radial nodes) was 0. This parent optical vortex beam was split into two daughter beams by a polarizing beam-splitting cube. A dove prism was placed in the path of one of the daughter beams to change the handedness of the beam with respect to the other daughter beam. In this way, the two daughter beams, which correspond to two separate vortex traps, will have opposing changes in their spatial intensity profile when the CGH is translated in a given direction. This opposite handedness in the spatial intensity profile of the two respective traps is important in bringing the trapped droplets together.

The presence of the dove prism caused an increase in the beam path of one of the beams, which in turn changed the focal plane of the resultant vortex trap. We corrected this difference by increasing the path length of the beam that did not go through the prism while monitoring the focal planes at which the two traps formed. The two daughter beams were recombined with a second polarizing beam-splitting cube, prior to sending them to the back aperture of the objective. During fusion, the CGH was translated laterally with respect to the laser beam to cause a change in the intensity distribution of the trap, which is seen as a shift in the location of the dark core (Figure 1B).

The CGH was microfabricated using standard photolithographic techniques, in which we first spin-coated the negative photoresist, SU-8, onto clean glass. The CGH pattern on a chrome photomask was then transferred onto SU-8 using photolithography and normal SU-8 processing procedures. The holographic pattern on the photomask was created by solving the wave equations[33−38] using MATLAB; the numerical output from MATLAB was then converted to a binary image, which was subsequently written onto a chrome blank to form the photomask.

Imaging Optical Intensity Profiles. Profiles of the optical vortex beams were taken with a laser profiler (BeamPro$_{filer}$ 2340, Photon Inc., San Jose, CA). Images of the vortex traps were obtained by monitoring the back-scattered laser light at the interface of the glass coverslip and water; the resultant intensity images were recorded using a high-sensitivity CCD camera. (Cascade 650, Roper Scientific Inc., Tucson, AZ).

Generation of an Emulsion of Aqueous Droplets. The refractive index of water and acetophenone is 1.33 and 1.53, respectively. An emulsion of water in acetophenone was made using a 10:1 ratio of acetophenone containing 0.0025% w/w sorbitan monooleate (SPAN 80) and distilled (DI) water. The mixture of water and acetophenone was shaken by hand for ∼5 s to generate the emulsion, which was used immediately. The emulsion was transferred by micropipette to PDMS wells placed on the microscope stage.

To form the PDMS wells that held the emulsion, a polystyrene petri dish was first filled halfway with a mixture of degassed PDMS prepolymer and catalyst. After curing in an oven for 6 h at 60 °C, the PDMS was diced into small pieces (10 mm × 10 mm). The center of each piece was punched using a cork punch (VWR), yielding a cylindrical well of 5 mm in diameter. The PDMS piece with the through hole was then conformally sealed to a coverslip and placed on top of the objective. It was necessary to cover the filled PDMS well with another coverslip to prevent contamination and instabilities due to evaporation or thermal fluctuation.

Desired droplets, with positions close to each other, were selected and trapped. During fusion the CGH was translated and the droplets moved toward each other to fuse, whereupon the traps were immediately turned off after coalescence.

Materials and Chemicals. Acetophenone and SPAN 80 were purchased from Sigma-Aldrich (St. Louis, MO). PDMS (Sylgard 184) was bought from Dow Corning Co. (Midland, MI). Gold Seal coverslips were from Erie Scientific (Portsmouth, NH), and polystyrene petri dishes were from BD Biosciences (San Jose, CA).

RESULTS AND DISCUSSION

Exclusion of Surrounding Aqueous Droplets by an Optical Vortex Trap. We formed two optical vortex traps by sending the TEM$_{00}$ output of the Nd:YAG laser through a CGH to generate a LG$_0^1$ beam, followed by splitting the LG$_0^1$ beam with a beam-

(33) Curtis, J. E.; Grier, D. G. *Opt. Lett.* **2003**, *28*, 872−874.
(34) Curtis, J. E.; Grier, D. G. *Phys. Rev. Lett.* **2003**, *90*.
(35) He, H.; Heckenberg, N. R.; Rubinszteindunlop, H. *J. Mod. Opt.* **1995**, *42*, 217−223.
(36) Lee, W. M.; Yuan, X. C.; Cheong, W. C. *Opt. Lett.* **2004**, *29*, 1796−1798.
(37) Basistiy, I. V.; Bazhenov, V. Y.; Soskin, M. S.; Vasnetsov, M. V. *Opt. Commun.* **1993**, *103*, 422−428.
(38) Bazhenov, V. Y.; Soskin, M. S.; Vasnetsov, M. V. *J. Mod. Opt.* **1992**, *39*, 985−990.
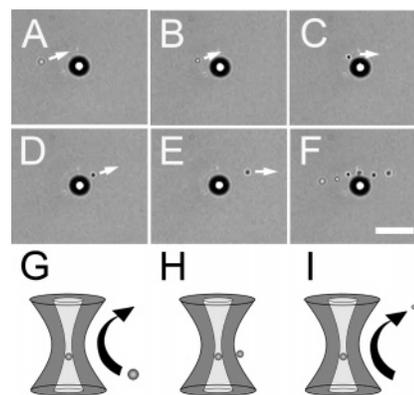
Figure 2. (A−E) A series of images that depict the repulsion and exclusion of a free-floating aqueous droplet (small droplet) from a vortex-trapped aqueous droplet (large droplet at the center of the image). The white arrows show the direction of movement of the small droplet that was being excluded from the vortex trap. (F) An overlay image that shows the trajectory of the small droplet as it was steered around the trapped droplet. (G−I) Schematics illustrating how an aqueous droplet that is outside of the vortex trap first impinges on the ring of laser light intensity that constitutes the vortex trap (G), then is stopped (H), and repelled (I) from the ring of light intensity. The scale bar in panel F represents 10 μm.

splitting cube (Figure 1A). An LG$_0^1$ beam is characterized by a helical phase distribution across the wavefront and a propagating phase singularity at the center. The phase singularity denotes a region of zero intensity, which is manifested as a dark core at the center of the plane orthogonal to the direction of beam propagation. The CGH creates the LG$_0^1$ beam from the TEM$_{00}$ output, with the practical outcome that when focused through a high NA objective, the balance of gradient and scattering forces from the ring of laser intensity allows objects with both low and high (relative to the medium) RI to be trapped (Figure 1C−E).

In the trapping of low-RI objects, such as aqueous droplets, the ring of laser intensity effectively forms a light cage that repels the trapped droplet and thus confines the droplet to the dark core. Similarly, this ring of laser intensity repels and excludes surrounding aqueous droplets and prevents them from entering the vortex trap. This characteristic is particularly useful when there is a high concentration of aqueous droplets dispersed in solution (such as in an emulsion), but only one droplet is to be manipulated and studied at a time. Because an optical vortex trap is stable in all three dimensions, the trapped droplet can be positioned precisely, as is seen with the two trapped droplets that were being positioned near each other for subsequent fusion (Figure 1E).

Figure 2 shows the repulsive effect of the vortex trap, where an aqueous droplet in the environment is displaced around the perimeter of a trapped droplet. This displacement is caused by a repulsive force generated in the region of high light intensity (Figure 2G−I), in the same manner and for the same reason as to why a conventional optical tweezer does not trap but will instead repel the droplet placed in the trap. The ability of the vortex trap to isolate the trapped droplet is useful, because this prevents uncontrolled droplet interactions and fusion and preserves the chemical content of the trapped droplet. For applications in single-cell or single-organelle analysis within encapsulating aqueous droplets, prevention of sample contamination and dilution through unwanted droplet fusion is particularly important.
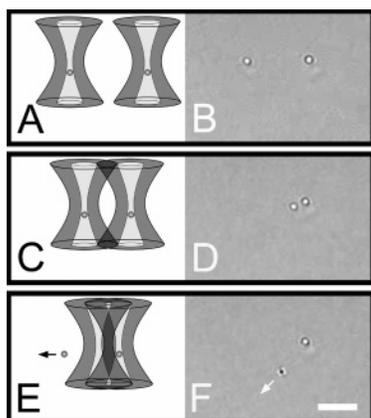
Figure 3. Schematic and images that illustrate the positioning and subsequent repulsion of two aqueous droplets in the dual vortex trap. (A–D) Two distant droplets were brought into close proximity; the schematic shows the positions of the two trapped droplets with respect to the positions of the rings of light intensity that form the dual vortex traps. (E, F) Repulsion that arose from the overlap of one of the droplets with the ring of light intensity that held the other droplet caused the loss of the droplet (white arrow indicates the direction of movement of the escaped droplet). The scale bar represents 10 μm.

Figure 4. Simulated and measured spatial intensity profiles for the optical vortex beam during the displacement of the hologram, which caused a lateral shift in embedded phase singularity or dark core. (A–D) shows the relative displacement of the laser beam (red spot) with respect to the dislocation in the hologram. (E–H) are simulations that show the resulting change in the intensity profile of the vortex beam. (I–P) are experimental measurements, where (I–L) are for the vortex beam that did not pass through the dove prism and (M–P) are for the beam that did pass through the dove prism.

Although the optical vortex trap is adept at trapping and translating single aqueous droplets, it is impaired in its ability to induce droplet fusion. The repulsive force imposed by the ring of light intensity that confines the aqueous droplet in the dark core also prevented two droplets from being brought together (Figure 3). As depicted in the schematics of Figure 3, in order for two droplets held in separate vortex traps to reach each other, they must cross through the highly intense region created by the overlap of the two traps. The result is that either one (Figure 3, parts E and F) or both droplets will be displaced by this overlap region of light intensity and lost to the traps. Without droplet fusion, the controlled initiation and mixing of different reagents from separate droplets is problematic.

Spatial Intensity Modulation of Optical Vortex Traps. One approach to overcome the repulsive effects of the vortex traps and to bring two aqueous droplets into close contact is to shift the position of the dark core with respect to the ring of laser intensity. This can be accomplished in principle by dynamically reconfiguring the holographic pattern that generates the LG_0^1 beam. With the use of spatial light modulators (SLMs), real-time changes to the holographic pattern can be made, although the controlled fusion of two aqueous droplets using SLMs still remains to be realized. While SLMs are flexible and provide a powerful platform to change the beam profiles dynamically, there are tradeoffs. First, SLMs have damage thresholds on the order of ~3 W/cm^2, which can limit the amount of power available for trapping. In comparison, our microfabricated hologram can withstand much higher incident laser intensities, at greater than 10^4 W/cm^2 as tested at the limit of our laser power output. In addition, SLMs are expensive. In return, SLMs are capable of much more complex real-time manipulations to the trapped particles than a static hologram.

Because our need to fuse two aqueous droplets represents relatively simple optical manipulations and because we need high powers to transport aqueous droplets in oil, which tends to be a much more viscous medium than water, we have decided to find
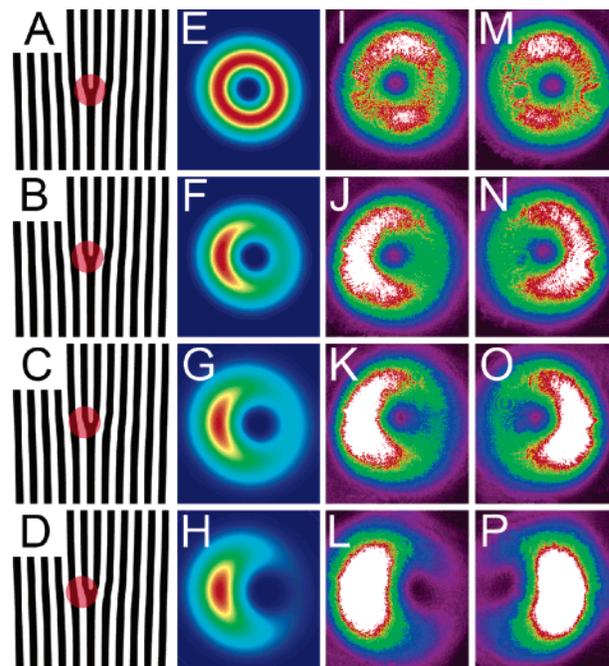
a simple method initially to induce droplet fusion based on microfabricated holograms and without resorting to SLMs. Our method is based on the finding that a lateral displacement of the CGH in a direction orthogonal to the beam-propagation axis can effect an asymmetric distribution of light intensity within the beam profile, while retaining the phase singularity (dark core) in the +-first-order diffracted field (Figure 4).[39–41]

Figure 4 shows our simulations and experimental measurements. The simulations (Figure 4, parts E–H) were performed by considering a special case of the electric field, an "off-axis vortex", which can be described by the following expression:

$$E(r,\varphi) = A \exp(-(r + r_0)^2/w_0^2) \cdot (\sqrt{2}r/w_0)\exp(iL\varphi) \tag{1}$$

where A is the amplitude of the peak intensity, w_0 is the waist of the beam, r and φ are in polar coordinates, L is 1, and r_0 is the displacement of the center of the Gaussian beam with respect to the center (i.e., the dislocation) of the CGH.

As the dark core is displaced laterally, the repulsive force from the high-intensity region of the light ring pushes the trapped aqueous droplet radially off-axis toward the direction of least

(39) Lee, W. M.; Ahluwalia, B. P. S.; Yuan, X. C.; Cheong, W. C.; Dholakia, K. *J. Opt. A* —Pure *Appl. Opt.* **2005**, *7*, 1–6.
(40) Tao, S. H.; Yuan, X. C.; Lin, J.; Peng, X.; Niu, H. B. *Opt. Exp.* **2005**, *13*, 7726–7731.
(41) Oemrawsingh, S. S. R.; Eliel, E. R.; Nienhuis, G.; Woerdman, J. P. *J. Opt. Soc. Am. A*—Opt., Image Sci., Vision **2004**, *21*, 2089–2096.
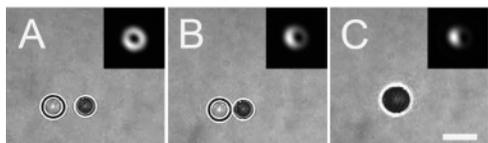
Figure 5. Images showing vortex-trap-induced fusion of two aqueous droplets in acetophenone (with 0.0025% w/w SPAN 80). The insets depict changes in the intensity profile of the vortex trap as the hologram was displaced; the images in the inset were obtained by recording the back-scattered laser light from the vortex trap off the interface between the coverslip and water. The scale bar represents 10 μm and applies to all panels.

intensity. The practical consequence is that the droplet will track the displacement of the dark core within the beam (Figure 4, parts I−P), which was instigated by the directional translation of the CGH.

In addition to changing the intensity profile of the optical vortex trap, the symmetry between the two traps needs to be changed. Otherwise, upon shifting of the dark core, the two trapped droplets will maintain a set distance between them as they are both moved in the same direction. We changed the handedness of one of the beams by sending it through a dove prism, which creates a mirror image of one trap with respect to the other. Figure 4 shows the intensity profiles of the two vortex beams as the CGH was displaced, where the third column (Figure 4, parts I−L) shows the beam without the prism and the fourth column (Figure 4, parts M−P) is the beam that has passed through the prism. The two dark cores now progress toward each other, enacting the movement and fusion of the aqueous droplets.

Vortex-Trap-Induced Fusion of Aqueous Droplets. The trapping and fusion of aqueous droplets was carried out with the following steps: (1) aqueous droplets were selected and trapped (Figure 5A), (2) the trapped droplets were positioned in close proximity with each other (Figure 5B), and (3) the dark core of each vortex trap was moved (see insets in Figure 5), causing the droplets to come into contact with each other and fuse (Figure 5C). Trapping power was between 100 and 300 mW for each trap

at the focal plane, with 300 mW giving better fusion because the repulsive force that pushed the droplets together was greater.

One point to consider is that the interfacial nature and stability of the droplet can affect the fusion success. We noticed that fusion became more difficult (i.e., required more laser power) with increased surfactant concentration, although one can overcome this issue by using more power in the traps. After droplet fusion, the modified traps could no longer hold the fused droplet in the longitudinal direction and pushed the droplet away along the z-direction. We addressed this issue by turning off the trap immediately after successful fusion. Because the droplet was in a low-Reynolds number environment, viscous retardation force immediately damped out the movement of the droplet upon shuttering the vortex trap. All that was needed to re-trap the fused droplet was to reset the CGH to its initial position. This process is amenable to automation and can be achieved easily with programmable electronic actuators and shutters.

CONCLUSION

The advantages of this droplet trapping and fusion technique lie in its capacity to trap aqueous droplets in any immiscible medium, protect trapped droplets from unwanted surrounding aqueous droplets, and initiate controlled droplet reactions. With on-demand vortex-trap-induced fusion, precise spatiotemporal control over the initiation of chemical reactions is possible. In combination with an appropriate microfluidic platform, this controlled vortex trapping and fusion technique for single droplets provides the degree of control, stability, and flexibility that is required for the detailed study of the small-volume phenomena that occur in femtoliter-volume droplets.